

# <sup>1</sup> Inferring Aerosol Forcing from Surface Temperature <sup>2</sup> Record

Yi Ming<sup>1</sup>

---

Yi Ming, Geophysical Fluid Dynamics Laboratory, Princeton, NJ 08542, USA.  
(Yi.Ming@noaa.gov)

<sup>1</sup>Geophysical Fluid Dynamics Laboratory,  
Princeton, NJ

3 **Abstract.** The Earth's surface temperature has risen by about 0.8 K over  
4 the last 100 years partly due to human activities. If not for the poorly un-  
5 derstood radiative effects of aerosols, one would have been able to better use  
6 the observed warming to constrain the all-important transient climate re-  
7 sponse (TCR, the pace of the warming caused by a continuous buildup of  
8 greenhouse gases). Here we show that it is feasible to infer the historical aerosol  
9 forcing and subsequently TCR from the surface temperature record by ex-  
10 ploiting the seasonality difference between the aerosol and greenhouse gas  
11 forcings. Our analysis suggests that the seasonally-varying aerosol forcing  
12 may have played a crucial role in causing the Northern Hemisphere (NH) win-  
13 ter to warm at a faster pace than the NH summer – a distinct feature of the  
14 observed warming. The estimated 25% to 75% range is  $-1.7 - -0.7 \text{ W m}^{-2}$   
15 for the aerosol forcing, and is  $0.9 - 1.7 \text{ K}$  (at the time of  $\text{CO}_2$  doubling) for  
16 TCR. The respective 5% to 95% ranges are  $-2.5 - 0.1 \text{ W m}^{-2}$  and  $0.7 - 3.8$   
17  $\text{K}$ . The median TCR of  $1.3 \text{ K}$  is considerably smaller than those projected  
18 with state-of-the-art climate models or derived in attribution studies. The  
19 results are highly relevant to shaping the climate outlook for the coming decades.

## 1. Introduction

As the near-term climate change is strongly tied to the transient climate response (TCR), the inability of climate models to converge on TCR hinders a reliable projection of future climate. (In this work, TCR is defined as the surface temperature change in response to a 1% year<sup>-1</sup> increase of CO<sub>2</sub> at the time of doubling.) The minimum and maximum values among the nineteen Intergovernmental Panel on Climate Change (IPCC) Fourth Assessment Report (AR4) models are 1.2 and 2.6 K, respectively, with a median of 1.6 K [Randall *et al.*, 2007]. (Note that this model ensemble does not provide an adequate sampling of model-simulated TCR, and the resulting range is particularly sensitive to outliers.) The inter-model spreads in cloud feedback and ocean heat uptake are among the main causes [Soden and Held, 2006; Winton *et al.*, 2001].

The alternative of inferring TCR from the past warming is plagued by the large uncertainty in the historical aerosol forcing [Andreae *et al.*, 2005]. The greenhouse gas forcing is 2.8 W m<sup>-2</sup> in the year 2010 (<http://www.esrl.noaa.gov/gmd/aggi/>), and the forcing associated with doubling CO<sub>2</sub> is 3.7 W m<sup>-2</sup>. One can write TCR approximately as  $3.7\delta T/(2.8 + F_a\epsilon)$ , where  $\delta T$  is the observed surface temperature change, and  $F_a$  and  $\epsilon$  are the aerosol forcing and its efficacy [Joshi *et al.*, 2003] (defined as the ratio of the climate sensitivity for a non-CO<sub>2</sub> forcing to that for CO<sub>2</sub>), respectively. [Note that this expression does not explicitly consider forcings other than greenhouse gases and aerosols (e.g., ozone, land use and solar), but their effects are likely to be small [Forster *et al.*, 2007].] The forward model estimates of a subset of known aerosol effects range from -2.2 to -0.5 W m<sup>-2</sup> [Forster *et al.*, 2007]. The implied TCR could vary considerably depending

41 on the estimated aerosol forcing. Unfortunately, process-level studies cannot rule out the  
42 possibility of a strong aerosol cooling and thus a large TCR [*Lohmann et al.*, 2010].

43 Is it possible to constrain the aerosol forcing and TCR simultaneously with the surface  
44 temperature record? If the surface temperature responses to aerosols and greenhouse gases  
45 possess sufficiently different patterns, their magnitudes can be quantified with the optimal  
46 fingerprinting approach by regressing the observed temperature anomalies on the changes  
47 caused by individual forcings [*Stott et al.*, 2006]. Hence the effectiveness of the approach  
48 hinges on one's ability to realistically simulate the latter. Particularly challenging for  
49 climate models is the surface temperature response to the aerosol forcing, which, due  
50 to its spatially and temporally inhomogeneity, is more effective at inducing circulation  
51 changes than well-mixed greenhouse gases [*Ming and Ramaswamy*, 2011], an issue that  
52 we will return to in the discussion section. This paper presents an attempt at separating  
53 the climate impacts of the two forcings by exploiting their difference in seasonality.

## 2. Seasonality of Aerosol Forcing

54 We use a modified version of the GFDL-AM2.1 model [*Ming and Ramaswamy*, 2009] and  
55 the GFDL-AM3 model [*Donner et al.*, 2011] to calculate the pre-industrial to present-day  
56 anthropogenic aerosol forcing, evaluated as radiative flux perturbation [*Haywood et al.*,  
57 2009]. Both direct (via scattering/absorbing solar radiation) and indirect effects (via en-  
58 hancing cloud albedo and lifetime) are included. Two models are different in cumulus  
59 parameterization, aerosol transport, aerosol optical properties and aerosol-cloud interac-  
60 tions. GFDL-AM2.1 is also used to compute the greenhouse gas forcing.

61 Fig. 1 shows the normalized monthly mean aerosol forcing simulated with two climate  
62 models. (Note that the normalized monthly mean forcing or insolation is calculated as

$(X_i - \bar{X})/\bar{X}$ , where  $X_i$  is the monthly mean for the  $i$ -th month and  $\bar{X}$  is the annual mean  
 ( $\sum_{i=1}^{12} X_i/12$ .) The seasonal cycle of the aerosol forcing – peaking in the boreal summer  
 and tapering off to a wintertime minimum – is remarkably consistent between the models  
 in spite of the numerous differences in model physics. Furthermore, it tracks closely the  
 seasonal cycle of the NH insolation. This is because anthropogenic aerosols are situated  
 primarily in the NH, and interact mainly with the shortwave (or solar) radiation. In  
 contrast, the greenhouse gas forcing, which affects the longwave (or terrestrial) radiation,  
 does not exhibit any seasonality. Assuming everything else being equal, one may speculate  
 that the seasonally-varying aerosol forcing would cool the NH summer more than the NH  
 winter. In the presence of a background greenhouse gas warming, aerosols would cause  
 the NH winter to warm more (or, in a transient sense, faster) than the NH summer. The  
 seasonality difference represents a physical mechanism through which the climate impacts  
 of aerosols and greenhouse gases can be potentially separated from each other.

### 3. Surface Temperature Record

This thinking leads us to examine the hemispheric seasonal warming trends using the  
 Goddard Institute for Space Studies (GISS) surface temperature analysis (GISTEMP)  
 [Hansen *et al.*, 2010]. We choose the analysis period of 1911-2010 for two reasons. First,  
 the data prior to 1911 may not be as reliable. Second, the 100-year span is long enough  
 to keep the role of natural variability relatively small. [Analyses for other periods (e.g.,  
 1881-2010 and 1941-2010) yield the same basic findings.] The least-squares linear trends  
 of the NH winter (December-January-February, denoted as  $\delta T_w$ ) and summer (June-July-  
 August, denoted as  $\delta T_s$ ) surface temperature are 0.89 and 0.61 K (100 years)<sup>-1</sup>, respec-  
 tively (Fig. 2), both of which are statistically significant at the 95% confidence level

85 based on the two-tailed Student's t-test [*Woodward and Gray, 1993; Santer et al., 2000*].  
 86 Stronger NH wintertime warming was also seen for other observational datasets [*Wallace*  
 87 *et al., 1995; Balling et al., 1998; Stine et al., 2009*].

88 Can one explain the seasonal contrast inherent in the observed warming by invoking  
 89 the natural fluctuations intrinsic to the climate system? We construct the cumulative  
 90 probability distribution of the seasonal difference in the unforced 100-year NH temperature  
 91 trend ( $\delta T_w - \delta T_s$ , denoted as  $\mathcal{T}$ ) from randomly sampling a 4000-year control simulation  
 92 performed with the GFDL-CM2.1 model [*Delworth and Coauthors, 2006*] (a Bootstrap  
 93 method [*Vecchi et al., 2006*]). The distribution is shown in the upper panel of Fig. 3. The  
 94 observed  $\mathcal{T}$  of  $0.27 \text{ K (100 years)}^{-1}$  lies outside the 95% confidence interval  $[-0.24 - 0.24$   
 95  $\text{K (100 years)}^{-1}]$ , suggesting that it is most likely forced by external forcings.

#### 4. Role of Greenhouse Gases

96 The more rapid NH wintertime warming has been discussed in the general context of  
 97 global warming [*Balling et al., 1998*]. This is, to a certain extent, consistent with the IPCC  
 98 AR4 model simulation of the climate response to a  $1 \text{ \% year}^{-1}$  increase of  $\text{CO}_2$ , which are  
 99 archived at the Program for Climate Model Diagnosis and Intercomparison (PCMDI) of  
 100 the US Department of Energy Lawrence Livermore National Laboratory (DOE/LLNL).  
 101 All the models agree that a steady rise in the greenhouse gas concentration would cause  
 102 the NH winter to warm at a faster pace than the NH summer. They, however, diverge  
 103 substantially in the strength of the effect. The normalized  $\mathcal{T}$  [ $2(\delta T_w - \delta T_s)/(\delta T_w + \delta T_s)$ ,  
 104 denoted as  $\tilde{\mathcal{T}}$ ] due to  $\text{CO}_2$  has a mean of 0.22 with a variance of 0.09 (the lower panel of  
 105 Fig. 3). The observed  $\tilde{\mathcal{T}}$  (0.37) deviates from the ensemble-mean by 0.15, which is only  
 106 slightly less than two variances. In addition, only one out of a total of seventeen models

107 yields a  $\tilde{\mathcal{T}}$  that is greater than the observation. These are strong indications that forcing  
 108 agents other than greenhouse gases may have also contributed to the seasonal difference  
 109 in the past warming. It is plausible to assume that, in light of its strong seasonality,  
 110 the aerosol forcing is responsible for the fraction of the observed seasonal difference that  
 111 cannot be accounted for by greenhouse gases.

## 5. A Conceptual Model of Aerosol Forcing

112 This argument motivates us to derive a mathematical expression for the historical  
 113 aerosol forcing. If the observed warming is driven entirely by greenhouse gases, the sea-  
 114 sonal difference in the NH warming ( $\mathcal{T}_g$ ) would be approximated as  $0.5\tilde{\mathcal{T}}_g(\delta T_w + \delta T_s)$ ,  
 115 where  $\tilde{\mathcal{T}}_g$  is the normalized  $\mathcal{T}$  in response to greenhouse gases alone and is estimated at  
 116  $0.22 \pm 0.09$  (one variance) from the IPCC AR4 model ensemble (the lower panel of Fig.  
 117 3). The influence of aerosols ( $\mathcal{T}_a$ ) is calculated as the residual of subtracting  $\mathcal{T}_g$  from the  
 118 observed  $\mathcal{T}$ .

119 The seasonal cycle of the solar input is the main driving force behind that of the surface  
 120 temperature. In the present climate state, the seasonal difference in the climatological NH  
 121 top-of-the-atmosphere solar absorption ( $\delta\mathbf{F}$ ) gives rise to a seasonal difference in the NH  
 122 surface temperature ( $\delta\mathbf{T}$ ). In an idealized climate state with time-invariant solar input,  
 123 the surface temperature would not vary temporally either. We assume that the climate  
 124 system, when being subjected to a change in the seasonal cycle of the solar input, would  
 125 behave linearly by following the slope set by the two states. It then follows that  $\mathcal{F}_a$ , which  
 126 is the seasonal difference in the NH aerosol forcing ( $F_{a,w} - F_{a,s}$ ), and can be thought of as a  
 127 perturbation to the solar input, is equal to  $\mathcal{T}_a\delta\mathbf{F}/\delta\mathbf{T}$ . (Because the phase of the seasonal  
 128 cycle of the surface temperature lags that of the solar input roughly by one month as

129 a result of thermal inertia, both  $\mathcal{F}_a$  and  $\delta\mathbf{F}$  contrast November-December-January with  
 130 May-June-July.)  $\delta\mathbf{F}$  is  $153.3 \text{ W m}^{-2}$  according to the 5-year Clouds and Earth's Radiant  
 131 Energy System (CERES) Energy Balanced and Filled (EBAF) dataset [Loeb *et al.*, 2009],  
 132 and  $\delta\mathbf{T}$  is 12 K according to the 30-year surface temperature climatology constructed by  
 133 the University of East Anglia Climate Research Unit (CRU) [Jones *et al.*, 1999]. The  
 134 respective variances owing to natural variations are estimated at  $0.4 \text{ W m}^{-2}$  and 0.1 K  
 135 (see SOM).

136 Because  $F_{a,s}$  is about 2.2 times of  $F_{a,w}$ ,  $\mathcal{F}_a$  is equal to  $1.2F_{a,w}$ . The NH annual mean  
 137 aerosol forcing, which can be evaluated as  $0.5(F_{a,w} + F_{a,s})$  or  $1.6F_{a,w}$ , is about  $1.3\mathcal{F}_a$ .  
 138 Since anthropogenic aerosols are mainly in the NH, the global mean aerosol forcing ( $F_a$ )  
 139 is approximately half of the NH forcing (i.e.,  $0.65\mathcal{F}_a$ ). We then arrive at a one-line equation  
 140 for  $F_a$ , which is  $0.65[(1 - 0.5\tilde{\mathcal{T}}_g)\delta T_w - (1 + 0.5\tilde{\mathcal{T}}_g)\delta T_s]\delta\mathbf{F}/\delta\mathbf{T}$ . The implied TCR can be  
 141 computed from  $F_a$  using the aforementioned equation [ $3.7\delta T/(2.8 + F_a\epsilon)$ ]. The forcing  
 142 efficacy ( $\epsilon$ ) is estimated at 0.7 with a variance of 0.05 [Forster *et al.*, 2007]. The observed  
 143 1911-2010 global mean surface temperature change ( $\delta T$ ) is 0.76 K based on GISTEMP.

144 Our method for determining the aerosol forcing and TCR is deterministic in nature.  
 145 The mean values of  $\delta T_w$ ,  $\delta T_s$  and  $\delta T$  are based on GISTEMP. Their natural variations  
 146 are estimated from randomly sampling the GFDL-CM2.1 control simulation described  
 147 above. The probability distributions of  $\tilde{\mathcal{T}}_g$  and  $\epsilon$  are assumed to be Gaussian. Monte  
 148 Carlo simulations are performed to generate the probability distributions of the aerosol  
 149 forcing and TCR.

150 Fig. 4 contains the probability distributions of the aerosol forcing (the upper panel) and  
 151 TCR (the lower panel) generated from propagating the natural variations in the surface



152 temperature changes ( $\delta T_w$ ,  $\delta T_s$  and  $\delta T$ ) and the estimated uncertainties in  $\tilde{\mathcal{T}}_g$ ,  $\delta \mathbf{F}$ ,  $\delta \mathbf{T}$  and  
153  $\epsilon$  through the equations derived above. The median value of  $F_a$  is  $-1.2 \text{ W m}^{-2}$ , with a 5%  
154 to 95% range of  $-2.5 - 0.1 \text{ W m}^{-2}$ . The values are generally consistent with the prevailing  
155 view that aerosols pose a net cooling effect on the climate. Our method for inferring  $F_a$   
156 does not explicitly preclude the possibility of an aerosol cooling that is strong enough to  
157 overwhelm the greenhouse gas warming. In that case, the net historical forcing would be  
158 negative, thereby implying a negative climate sensitivity. The method is well-behaved in  
159 the sense that no solution resides in this unphysical regime. It is also reassuring to see that  
160 our results agree broadly with the forward climate model calculations (a median of  $-1.3 \text{ W}$   
161  $\text{m}^{-2}$  and a 5% to 95% range of  $-2.2 - -0.5 \text{ W m}^{-2}$ ) [*Forster et al.*, 2007]. Nonetheless, this  
162 agreement should be interpreted with caution as the two sets of results are not directly  
163 comparable. For example, the former implicitly accounts for all aerosol effects, while the  
164 latter considers only a subset.

165 The probability distribution of TCR is skewed heavily toward the low end (less than 1  
166 K), with a long tail extending to 3 – 4 K. This distribution reflects the fact that TCR is  
167 inversely proportional to the net historical forcing, and the latter (or the aerosol forcing)  
168 is determined independently of TCR in our method. The 90% confidence interval of 0.7  
169 – 3.8 K is slightly wider than the likely range of 1 – 3.5 K given in AR4 [*Hegerl et al.*,  
170 2007], and encompasses those of individual attribution studies [*Stott et al.*, 2006; *Forest*  
171 *et al.*, 2006; *Knutti and Tomassini*, 2008; *Gregory and Forster*, 2008; *Gillett et al.*, 2011;  
172 *Libardoni and Forest*, 2011; *Padilla et al.*, 2011]. The probability distributions, however,  
173 are very different. Our median TCR of 1.3 K is significantly smaller than the previously  
174 reported values (i.e., 2.1 K [*Stott et al.*, 2006], 1.9 K [*Forest et al.*, 2006] and 1.6 K [*Knutti*

175 *and Tomassini, 2008*]). It is even smaller than the 5% percentiles of most existing studies  
 176 [*Stott et al., 2006; Forest et al., 2006; Gregory and Forster, 2008; Gillett et al., 2011;*  
 177 *Padilla et al., 2011*]. A series of sensitivity experiments are used to assess how the results  
 178 may vary with the estimated natural variations in the surface temperature trends and  
 179 the estimated uncertainties in  $\tilde{\mathcal{T}}_g$  and  $\epsilon$ . Halving the estimated natural variations in  $\delta T_w$   
 180 and  $\delta T_s$  (Sensitivity Case #1) reduces the 95% percentile to 2.5 K, while halving the  
 181 estimated uncertainty in  $\tilde{\mathcal{T}}_g$  (Sensitivity Case #2) decreases it to 2.8 K. (Note that the  
 182 natural variations in the UKMO-HadCM3 model are about half of those in the GFDL-  
 183 CM2.1.) Neither the 5% percentile nor the median is substantially changed in these  
 184 sensitivity experiments. This indicates that the low end of the estimated TCR is rather  
 185 robust.

## 6. Discussion

186 Our results indicate that the magnitudes of the aerosol forcing and TCR may have  
 187 been systematically overestimated in the attribution studies. As explained before, the  
 188 fingerprinting approach employed in these studies relies heavily on the model-simulated  
 189 surface temperature response to aerosols. The inter-hemispheric asymmetry in the aerosol  
 190 forcing tends to prompt a net cross-equatorial energy transport, which acts to compensate  
 191 for the NH radiative cooling, and in doing so, spread its impact to the Southern Hemi-  
 192 sphere [*Ming and Ramaswamy, 2011*]. It has been shown, however, that the degree of the  
 193 compensation varies considerably with some highly uncertain aspects of model physics  
 194 such as cumulus parameterization and cloud feedback [*Kang et al., 2008*]. In some of the  
 195 AR4 historical simulations, the NH warms much less than the SH. This is contrary to the  
 196 observations, and appears to indicate that the aerosol-induced cooling is to a large extent

197 confined within the NH due to rather weak compensation in those models. Given that  
198 the NH/SH contrast in warming has been deemed particularly important for constraining  
199 the aerosol forcing [*Stott et al.*, 2006], the discrepancies among models in the response to  
200 an asymmetric forcing would render some of them unfit for being used to detect aerosols.

201 In comparison, our method for separating the climate impacts of aerosols and green-  
202 house gases is based primarily on a physically sound mechanism, namely the seasonality  
203 difference between two forcings. Unlike the fingerprinting approach, it does not use the  
204 model-simulated response to aerosols. Adding to the evidence of serious model deficiency  
205 in simulating the response to aerosols is the fact that the AR4 models generally cannot  
206 capture the observed changes in the amplitude and phase of the seasonal cycle [*Stine*  
207 *et al.*, 2009]. This raises the doubt that the attribution studies based on these models  
208 may be unable to take into account the mechanism identified here.

209 We conclude by emphasizing that our method, which is broad-brush in nature, involves  
210 a number of assumptions. Chief among them is that the aerosol-induced change in the  
211 seasonal cycle would follow the same proportionality constant as the full seasonal cycle  
212 itself. One cannot discount the possibility that the seasonal cycle may respond differently  
213 to the inhomogeneous aerosols and to the relatively smooth insolation. Unfortunately, we  
214 cannot use existing climate models to test this assumption due to their aforementioned  
215 deficiencies in capturing many aspects of the climate response to aerosols.

216 **Acknowledgments.** We thank Isaac Held, V. Ramaswamy and Michael Winton for reviewing  
217 an earlier version of the paper.

## References

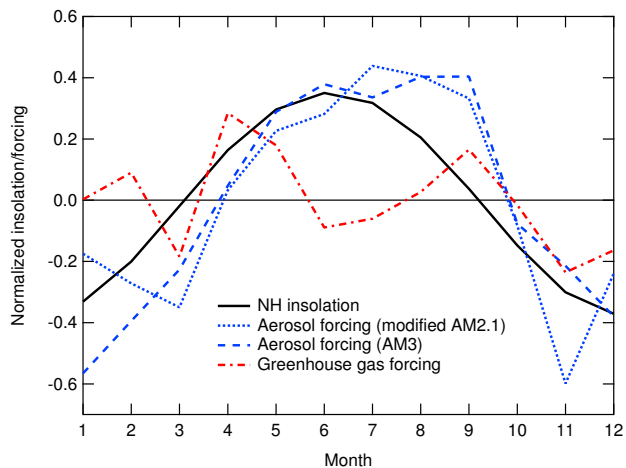
- 218 Andreae, M. O., C. D. Jones, and P. M. Cox (2005), Strong present-day aerosol cooling implies  
219 a hot future, *Nature*, *435*, 1187–1190.
- 220 Balling, R. C., P. J. Michaels, and P. C. Knappenberger (1998), Analysis of winter and summer  
221 warming rates in gridded temperature time series, *Clim. Res.*, *9*, 175–181.
- 222 Delworth, T. L., and Coauthors (2006), GFDL’s CM2 global coupled climate models. Part I:  
223 Formulation and simulation characteristics, *J. Clim.*, *19*, 643–674.
- 224 Donner, L. J., et al. (2011), The dynamical core, physical parameterizations, and basic simulation  
225 characteristics of the atmospheric component of the GFDL global coupled model CM3, *J. Clim.*,  
226 *24*, 3484–3519.
- 227 Forest, C. E., P. H. Stone, and A. P. Sokolov (2006), Estimated PDFs of climate sys-  
228 tem properties including natural and anthropogenic forcings, *Geophys. Res. Lett.*, *33*, doi:  
229 10.1029/2005GL023977.
- 230 Forster, P., et al. (2007), Changes in atmospheric constituents and in radiative forcing, in *Climate*  
231 *Change 2007: The Physical Science Basis. Contribution of Working Group I to the Fourth*  
232 *Assessment Report of the Intergovernmental Panel on Climate Change*, edited by S. Solomon,  
233 D. Qin, M. Manning, Z. Chen, M. Marquis, K. B. Averyt, M. Tignor, and H. L. Miller,  
234 Cambridge University Press, Cambridge, United Kingdom and New York, NY, USA.
- 235 Gillett, N., V. K. Arora, G. M. Flato, J. F. Scinocca, and K. von Salzen (2011), Improved  
236 constraints on 21st-century warming derived using 160 years of temperature observations,  
237 *Geophys. Res. Lett.*
- 238 Gregory, J. M., and P. M. Forster (2008), Transient climate response estimated from radiative  
239 forcing and observed temperature change, *J. Geophys. Res.*, *113*, doi:10.1029/2008JD010405.

- 240 Hansen, J., R. Ruedy, M. Sato, and K. Lo (2010), Global surface temperature change, *Rev.*  
241 *Geophys.*, *48*, doi:10.1029/2010RG000345.
- 242 Haywood, J. M., L. J. Donner, A. Jones, and J.-C. Golaz (2009), Global indirect radiative forcing  
243 caused by aerosols: IPCC (2007) and beyond, in *Clouds in the Perturbed Climate System*, edited  
244 by J. Heintzenberg and R. Charlson, MIT Press, Cambridge, MA, USA.
- 245 Hegerl, G. C., F. W. Zwiers, P. Braconnot, N. P. Gillett, Y. Luo, J. A. M. Orsini, N. Nicholls,  
246 J. E. Penner, and P. A. Stott (2007), Understanding and attributing climate change, in *Climate*  
247 *Change 2007: The Physical Science Basis. Contribution of Working Group I to the Fourth*  
248 *Assessment Report of the Intergovernmental Panel on Climate Change*, edited by S. Solomon,  
249 D. Qin, M. Manning, Z. Chen, M. Marquis, K. B. Averyt, M. Tignor, and H. L. Miller,  
250 Cambridge University Press, Cambridge, United Kingdom and New York, NY, USA.
- 251 Jones, P., M. New, D. E. Parker, S. Martin, and I. G. Rigor (1999), Surface air temperature and  
252 its variations over the last 150 years, *Rev. Geophys.*, *37*, 173–199.
- 253 Joshi, M., K. Shine, M. Ponater, N. Stuber, R. Sausen, and L. Li (2003), A comparison of  
254 climate response to different radiative forcings in three general circulation models: Towards  
255 an improved metric of climate change, *Clim. Dyn.*, *20*, 843–854.
- 256 Kang, S. M., I. M. Held, D. M. W. Frierson, and M. Zhao (2008), The response of the ITCZ  
257 to extratropical thermal forcing: Idealized slab-ocean experiments with a GCM, *J. Clim.*, *21*,  
258 3521–3532.
- 259 Knutti, R., and L. Tomassini (2008), Constraints on the transient climate response from observed  
260 global temperature and ocean heat uptake, *Geophys. Res. Lett.*, *35*, doi:10.1029/2007GL032904.
- 261 Libardoni, A. G., and C. E. Forest (2011), Sensitivity of distributions of climate system properties  
262 to the surface temperature dataset, *Geophys. Res. Lett.*, *38*, doi:10.1029/2011GL049431.

- 263 Loeb, N. G., B. A. Wielicki, D. R. Doelling, G. L. Smith, D. F. Keyes, S. Kato, N. Manalo-  
264 Smith, and T. Wong (2009), Toward optimal closure of the Earth's top-of-atmosphere radiation  
265 budget, *J. Clim.*, *22*, 748–766.
- 266 Lohmann, L. R. U., T. Storelvmo, A. Jones, S. Menon, J. Quaas, A. Ekman, D. Koch, and  
267 R. Ruedy (2010), Total aerosol effect: radiative forcing or radiative flux perturbation?, *Atmos.*  
268 *Chem. Phys.*, *10*, 3235–3246.
- 269 Ming, Y., and V. Ramaswamy (2009), Nonlinear climate and hydrological responses to aerosol  
270 effects, *J. Clim.*, *22*, 1329–1339.
- 271 Ming, Y., and V. Ramaswamy (2011), A model investigation of aerosol-induced changes in trop-  
272 ical circulation, *J. Clim.*, *24*, 5125–5133.
- 273 Padilla, L. E., G. K. Vallis, and C. W. Rowley (2011), Probabilistic estimates of transient climate  
274 sensitivity subject to uncertainty in forcing and natural variability, *J. Clim.*, *24*, doi:5521-5537.
- 275 Randall, D., et al. (2007), Climate models and their evaluation, in *Climate Change 2007: The*  
276 *Physical Science Basis. Contribution of Working Group I to the Fourth Assessment Report of*  
277 *the Intergovernmental Panel on Climate Change*, edited by S. Solomon, D. Qin, M. Manning,  
278 Z. Chen, M. Marquis, K. B. Averyt, M. Tignor, and H. L. Miller, Cambridge University Press,  
279 Cambridge, United Kingdom and New York, NY, USA.
- 280 Santer, B. D., T. M. L. Wigley, J. S. Boyle, D. J. Gaffen, J. J. Hnilo, D. Nychka, D. E.  
281 Parker, and K. E. Taylor (2000), Statistical significance of trends and trend differences in  
282 layer-average atmospheric temperature time series, *J. Geophys. Res.*, *105*, 7337–7356, doi:  
283 10.1029/1999JD901105.
- 284 Soden, B. J., and I. M. Held (2006), An assessment of climate feedbacks in coupled ocean-  
285 atmosphere models, *J. Clim.*, *19*, 3354–3360.

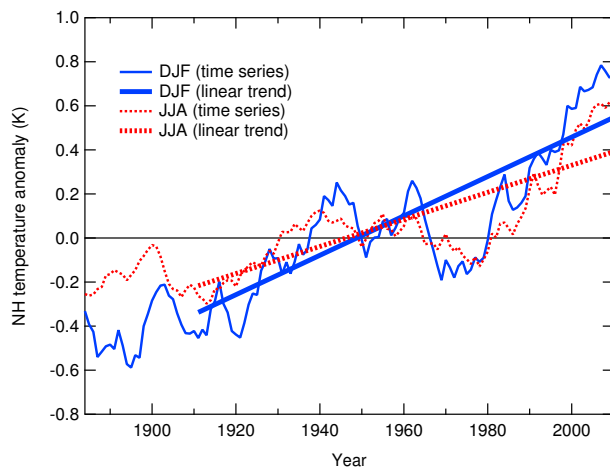
- 286 Stine, A. R., P. Huybers, and I. Y. Fung (2009), Changes in the phase of the annual cycle of  
287 surface temperature, *Nature*, *457*, 435–440.
- 288 Stott, P. A., J. F. B. Mitchell, M. R. Allen, T. L. Delworth, J. M. Gregory, G. A. Meehl, and  
289 B. D. Santer (2006), Observational constraints on past attributable warming and predictions  
290 of future global warming, *J. Clim.*, *19*, 3055–3069.
- 291 Vecchi, G. A., B. J. Soden, A. T. Wittenberg, I. M. Held, A. Leetmaa, and M. J. Harrison (2006),  
292 Weakening of Tropical Pacific atmospheric circulation due to anthropogenic forcing, *Nature*,  
293 *441*, 73–76.
- 294 Wallace, J. M., Y. Zhang, and J. A. Renwick (1995), Dynamic contribution to hemispheric mean  
295 temperature trends, *Science*, *270*, 780–783.
- 296 Winton, M., K. Takahashi, and I. M. Held (2001), Importance of ocean heat uptake efficacy to  
297 transient climate change, *J. Clim.*, *17*, 845–856.
- 298 Woodward, W., and H. Gray (1993), Global warming and the problem of testing for trend in  
299 time series data, *J. Clim.*, *6*, 953–962.

Figure 1. Normalized monthly mean forcing or insolation.





**Figure 2.** 5-year running means of the NH seasonal surface temperature anomalies (solid lines) and the corresponding least-squares linear trends (dotted lines).



**Figure 3.** Cumulative probability distribution of the seasonal difference in the unforced 100-year NH temperature trend created from randomly sampling a 4000-year control simulation (the upper panel) and the normalized seasonal difference in the CO<sub>2</sub>-induced warming (the lower panel).

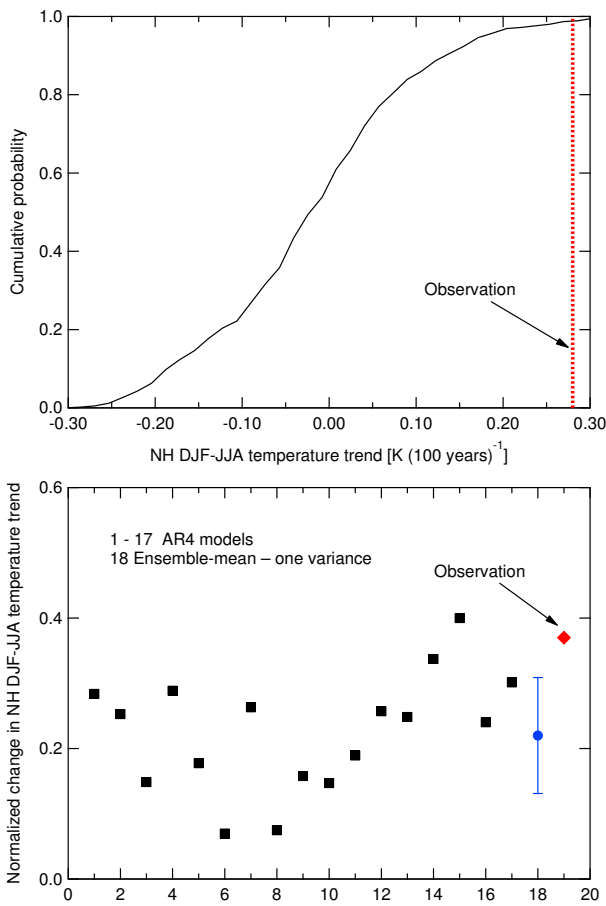


**Figure 4.** Probability distributions of the inferred aerosol forcing (the upper panel) and transient climate response (the lower panel). See the text for the description of the sensitivity cases. The horizontal bars represents the 5% to 95% ranges.

